Spectrochimica Acta Part A: Molecular and Biomolecular Spectroscopy 118 (2014) 897–902

Contents lists available at ScienceDirect

Spectrochimica Acta Part A: Molecular and Biomolecular Spectroscopy

journal homepage: www.elsevier.com/locate/saa

Study on the interaction between histidine-capped Au nanoclusters and bovine serum albumin with spectroscopic techniques

Chengzhi Zheng, Huiping Wang, Wei Xu, Chaoyong Xu, Jiangong Liang *, Heyou Han

State Key Laboratory of Agricultural Microbiology, College of Science, Institute of Chemical Biology, Huazhong Agricultural University, Wuhan 430070, PR China

HIGHLIGHTS

- The interaction of histidine-capped Au nanoclusters with BSA was investigated.
- Au nanoclusters quenched the fluorescence of BSA by a dynamic style.
- The interaction was driven by hydrophobic force.
- Au nanoclusters altered the molecular structure of BSA.

GRAPHICAL ABSTRACT

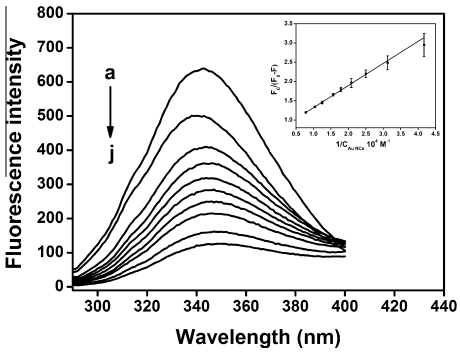

ARTICLE INFO

Article history:
Received 17 April 2013
Received in revised form 11 August 2013
Accepted 25 September 2013
Available online 7 October 2013

Keywords:
Au nanoclusters
Bovine serum albumin
Interaction
Quenching
Fluorescence

ABSTRACT

The understanding of the protein-nanoclusters interaction has significant implications for biological applications of nanoclusters (NCs). In this manuscript, the interaction of histidine-capped Au nanoclusters (NCs) with bovine serum albumin (BSA) has been investigated by fluorescence, UV–vis, circular dichroism (CD) and Raman spectroscopic techniques under simulative physiological conditions. The results showed that the fluorescence of BSA was quenched by Au NCs. The quenching mechanism was discussed to be a dynamic quenching style, which was proved by the fluorescence spectra and UV–vis absorption spectra. According to modified Stern–Volmer equations at different temperatures, corresponding thermodynamic parameters, ΔH^{θ}, ΔS^{θ} and ΔG^{θ} were observed to be 35.97 kJ mol^{-1}, 199.53 J mol^{-1} K^{-1} and −23.49 kJ mol^{-1}, respectively. The hydrophobic force played a key role in the interaction process. Further results from the CD spectra and Raman spectra demonstrated that the α-helical content in BSA was reduced upon interaction with Au NCs which induced a partial protein destabilization. This study contributes to a better understanding of the biology toxicity of Au NCs to biomolecular, which is very essential for the development of safe and functional Au NCs.

Introduction

Noble metal nanoclusters (NCs), composed of a few to roughly a hundred atoms, have arisen as a novel type of fluorescent nanomaterials in recent years [1,2]. These NCs provide the "missing link" between atomic and nanoparticle behaviors, and have consequently attracted a great deal of attention [3,4]. Among the various noble metal NCs, Au NCs have been the subject of intense interest, owing to their good biocompatibility, extraordinary stability, and facile synthesis [5]. Indeed, recent studies have demonstrated the usefulness of fluorescent Au NCs in biodetection and bioimaging, such as biomolecule detection [6], intracellular metal ion sensing [7], living cell labeling [8] and in vivo imaging [9].

Notwithstanding their excellent advantages, Au NCs may cause undesirable hazardous interactions with biological systems and the environment with potential to generate toxicity. Therefore, it is very crucial to explore the interactions between Au NCs and

* Corresponding author. Tel.: +86 27 87283712; fax: +86 27 87282133.
E-mail address: liangjg@mail.hzau.edu.cn (J. Liang).

1386-1425/$ - see front matter © 2013 Elsevier B.V. All rights reserved.
http://dx.doi.org/10.1016/j.saa.2013.09.082

biological systems, such as biomolecule, cell and in vivo. Although great progress on the effects of Au NCs on cell and in vivo has been made [9–12], knowledge of their interaction with biomolecules is still limited [13]. Therefore, a better understanding of the interaction between biomolecules and Au NCs is very essential for the development of functional and safe Au NCs.

Owing to its structural homology with human serum albumin (HSA), bovine serum albumin (BSA) has been one of the most extensively studied proteins [14]. It is the most abundant protein in blood plasma and plays an important role in the transport of numerous endogenous ligands, metabolites, hormones, anesthetics and other commonly used drugs [15]. As a model protein, BSA has two tryptophans, Trp-134 and Trp-212 [16], which possess intrinsic fluorescence and have commonly been utilized to study the interactions between nanoparticles and biomolecules [17–19].

In this work, the interaction between histidine-capped Au NCs and BSA was probed according to the effect of Au NCs on the fluorescence of BSA. The interaction information of Au NCs with BSA such as the quenching mechanism, the interaction forces and conformational changes of BSA was provided based on the spectroscopic techniques. This report provides a new approach to explore the potential biological toxicity of Au NCs at the functional macrobiomolecular level.

Experimental

Chemicals

Bovine serum albumin (BSA), $HAuCl_4{\cdot}4H_2O$ and histidine were purchased from Sinopharm Chemical Reagent Co., Ltd. The other common chemicals were obtained from commercial sources. All reagents were of analytical reagent grade and used without further purification. Ultrapure water was used throughout.

Apparatus

The UV–vis absorption spectra were obtained with 1.0 cm × 1.0 cm quartz cuvette on a Thermo Nicolet Corporation Model evolution 300 UV–vis spectrometer (America). All fluorescence spectra were recorded by a Shimadzu RF-5301PC Spectrofluorometer (Japan) equipped with a 20 kW xenon discharge lamp as a light source. Fluorescence lifetime measurements were performed via a FLS920-st Steady State and TCSPC Fluorescence Lifetime Spectro-Fluorimeter from Edinburgh Instruments Ltd. The Raman spectra were acquired with an in via micro-Raman spectroscopy system (Renishow, UK) in a spectral range of 500–2000 cm^{-1}, equipped with a He–Ne laser excitation source emitting wavelength at 633 nm. The CD spectra were recorded on a Jasco (J-810) automatic recording spectropolarimeter, using a cylindrical cuvette of 0.1 cm path length.

The synthesis of histidine-capped Au NCs

The Au NCs were synthesized in one pot following the method developed by Yang et al. [20]. Briefly, an aqueous solution of $HAuCl_4$ (1.00 mL, 10 mM) was mixed with an aqueous solution of histidine (3.00 mL, 100 mM) in a small vial at room temperature. The mixture was incubated for 2 h and the color turned pale yellow, indicating the formation of Au NCs.

The effect of Au NCs on the fluorescence of BSA

For the fluorescence measurement, BSA concentration was kept at 5.00×10^{-7} M and Au NCs concentration varied. Fluorescence spectra were recorded at 298 K, 304 K and 310 K in the range of 290–400 nm upon excitation at 280 nm in each case.

Results and discussion

Characterization of as-prepared Au NCs

Fig. 1 depicted the UV–vis absorption and fluorescence emission spectra of histidine protected Au NCs. It can be seen that the absorption spectrum of Au NCs shows an obvious peak at 256 nm, which misses the characteristic surface plasmon resonance peak of Au nanoparticles (NPs), indicating the absence of Au NPs in the synthesis process. The fluorescence spectrum possesses an emission maximum at 481 nm, which is basically in line with the result in literature [20]. Obviously, the synthesis of Au NCs promises ideal results of the subsequent experiments. The concentration of Au NCs was calculated according to a Ref. [21].

The fluorescence quenching mechanism

The effect of Au NCs on BSA fluorescence intensity was shown in Fig. 2A. When different amounts of histidine-capped Au NCs solution were added to a fixed concentration of BSA, a remarkable decrease in the fluorescence intensity of BSA was observed. Meanwhile, we have evaluated the influence of histidine on BSA. Fig. 2B demonstrated that the fluorescence intensity of BSA was not affected by histidine even at a concentration as high as 3.84×10^{-2} M. These results definitely indicated that the fluorescence of BSA was quenched by histidine-capped Au NCs rather than histidine.

Taking into account of the inner-filter effect in the quenching process, we have adopted the following equation to correct the fluorescence intensity of BSA [22].

$$F_{corr} = F_{obs} \times 10^{(Aexc+Aem)/2} \quad (1)$$

where F_{corr} and F_{obs} are the corrected and observed fluorescence intensity of BSA, A_{exc} and A_{em} are the absorption value of the system at the excitation wavelength and emission wavelength, respectively. All the fluorescence intensities and spectra used below in this paper are the corrected fluorescence. The fluorescence quenching data were analyzed by the Stern–Volmer equation:

$$F_0/F = 1 + K_{sv}[Q] \quad (2)$$

where F_0 and F are the fluorescence intensities of BSA in the absence and presence of Au NCs, respectively. K_{SV} is the Stern–Volmer quenching constant, which is a measure of the quenching efficiency, and [Q] is the concentration of Au NCs. The plot of F_0/F versus [Q]

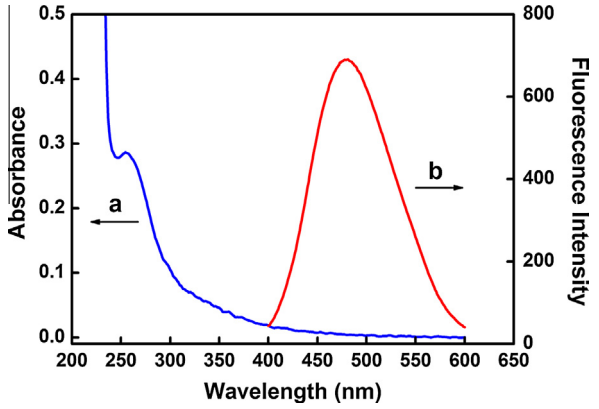

Fig. 1. UV–vis absorption (a) and fluorescence emission (b) spectra (λ_{ex} = 386 nm) of histidine-capped Au NCs. The concentration of Au NCs was 6.67×10^{-5} M.

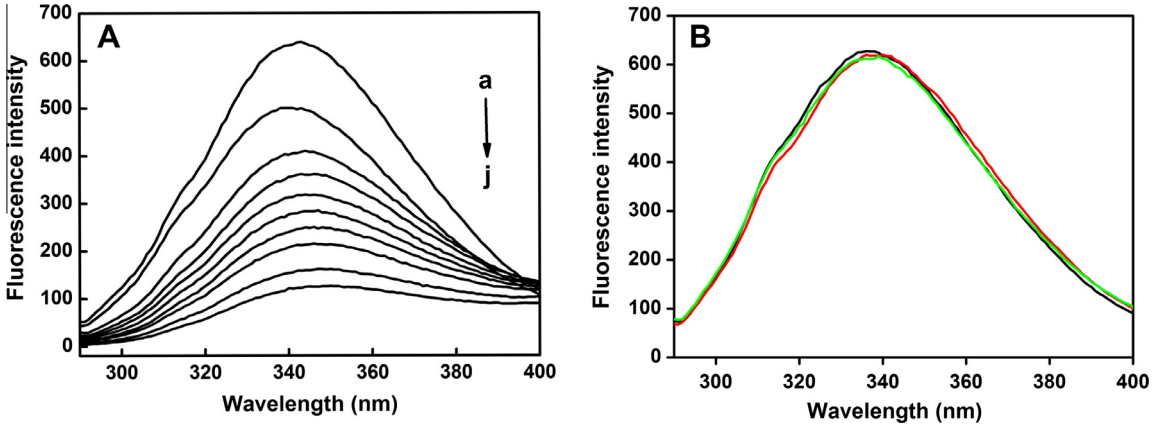

Fig. 2. Fluorescence spectra of BSA in the prescence of histidine-capped Au NCs (A) and histidine (B) at 0.01 M PBS (pH = 7.4). BSA concentration was fixed at 5.00×10^{-7} M. Au NCs concentrations were (a) 0, (b) 2.40, (c) 3.20, (d) 4.00, (e) 4.80, (f) 5.60, (g) 6.40, (h) 8.00, (i) 9.60, (j) 12.80×10^{-5} M. Histidine concentrations were 0 (black line), 1.20×10^{-2} M (red line) and 3.84×10^{-2} M (green line) ($\lambda_{ex} = 280$ nm). (For interpretation of the references to color in this figure legend, the reader is referred to the web version of this article.)

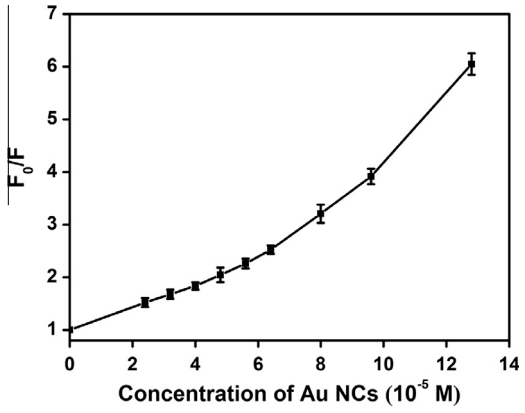

Fig. 3. Stern–Volmer curves of F_0/F versus concentration of Au NCs at 298 K at 0.01 M PBS (pH = 7.4). The concentration of BSA was fixed at 5.00×10^{-7} M.

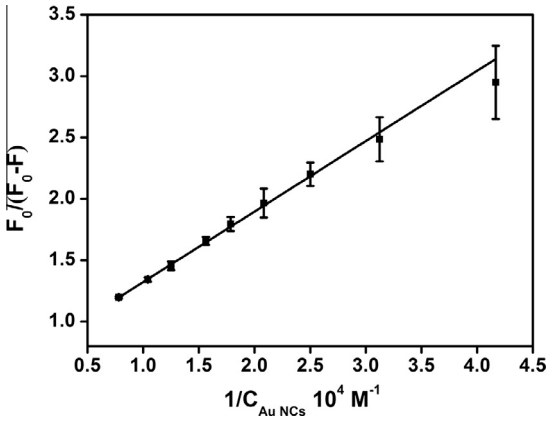

Fig. 4. The modified Stern–Volmer curves of $F_0/(F_0 - F)$ versus concentration of Au NCs at 298 K at 0.01 M PBS (pH = 7.4). The concentration of BSA was fixed at 5.00×10^{-7} M.

(Fig. 3) showed a positive deviation (concave towards the y axis), indicating the presence of both static and dynamic quenching.

The fluorescence data obtained at 298 K, 304 K and 310 K were further examined using the modified Stern–Volmer equation:

$$F_0/(F_0 - F) = 1/f_a + 1/(f_a K'_{sv}[Q]) \quad (3)$$

where F_0 and F are the corrected fluorescence intensity of BSA in the absence and prescence of Au NCs at concentration $[Q]$, f_a is the molar fraction of solvent-accessible BSA and K'_{SV} is the effective quenching constant for the accessible BSA. From the plot of $F_0/(F_0 - F)$ versus $1/[Q]$ (Fig. 4), the values of f_a and K'_{SV} were obtained. The value of f_a was observed to be 1.33 at 298 K, showing that 75.2% of the total fluorescence of BSA was accessible to the quencher (Au NCs) [23]. The K'_{SV} was found to be 1.31×10^4 M^{-1} at 298 K, which is ca. five orders of magnitude lower than that of Au NPs [24]. The low quenching efficiency of these ultrasmall Au NCs can be rationalized by the strong size dependence [19,21]; smaller metal particles quench the emission of adjacent fluorophores less efficiently. The results also showed the quenching constant K'_{SV} was positively correlated with the temperature. As we all know, for static quenching, the stability of complex formation will decrease with increasing temperature, causing the quenching constant K'_{SV} to be inversely correlated with the temperature. Thus, these results suggested that the quenching mechanism was dynamic.

UV–vis absorption measurement is a very simple method and applicable to explore the structural changes of the complex formation [25]. Herein, we have recorded the UV–vis absorption spectra of BSA (Fig. 5a), Au NCs (Fig. 5b) and BSA-Au NCs mixture (Fig. 5c), respectively. The absorption spectrum of the mixture (Fig. 5c) was identical with the mathematical superposition of absorption spectra of BSA and Au NCs (Fig. 5d). Since the complex

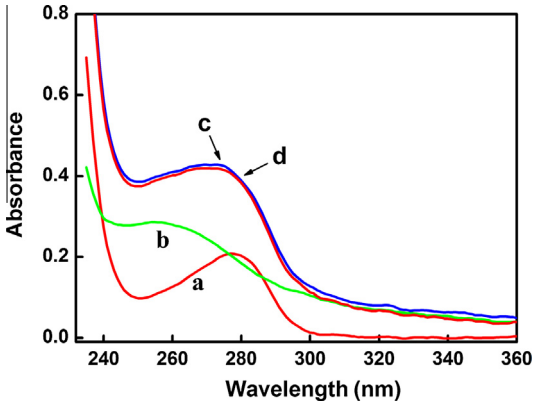

Fig. 5. The UV–vis absorption spectra of (a) BSA, (b) Au NCs, (c) BSA–Au NCs and (d) the mathematical superposition of BSA and Au NCs. The concentrations of BSA and Au NCs were 5.00×10^{-6} M and 1.00×10^{-4} M, respectively.

formation from static quenching usually results in a change in the absorption spectra, the unchangeable absorption spectra in this study suggested that the quenching style between Au NCs and BSA was dynamic rather than static.

To further verify the quenching style is dynamic but not static, we have measured the fluorescence lifetime of BSA in the absence and prescence of Au NCs. Fig. 6 represented the fluorescence decay curves of BSA at different concentrations of Au NCs. The fluorescence lifetime of BSA (concentration 2.00×10^{-5} M) decreased from 7.43 ns to 6.93 ns and 6.42 ns upon interaction with Au NCs (concentration 1.00×10^{-4} M and 2.00×10^{-4} M), respectively. As reported by Lakowicz [23], for a static quenching, the complex formation will not disturb the fluorescence lifetime of BSA. However, the fluorescence lifetime will be cut down due to the collision between the excited BSA and Au NCs in a dynamic quenching procedure. Consequently, the results unambiguously confirmed that the dynamic quenching was dominant in this reaction process.

The determination of the force acting between Au NCs and BSA

Generally, the interaction between endogenous or exogenous ligands and biological macromolecules is a complex process that involves electrostatic interactions, van der Waals force, multiple hydrogen bonds, π–π stacking, hydrophobic and so forth [26]. As well known, all chemical, physical, and biological processes are accompanied by a change in thermodynamic parameters (ΔG^{θ}, ΔH^{θ}, and ΔS^{θ}) [27]. Thus, to study the interaction between BSA and Au NCs, the thermodynamic parameters were calculated. If ΔH^{θ} is temperature independent in the temperature range studied [28], both ΔH^{θ} and ΔS^{θ} can be calculated from the following equation:

$$\ln K^{\theta} = -\Delta H^{\theta}/(RT) + \Delta S^{\theta}/R \quad (4)$$

where ΔH^{θ} and ΔS^{θ} are the standard enthalpy and entropy change for the reaction, respectively. R is the gas constant 8.314 J mol^{-1} K^{-1} and T is the temperature (K) and K^{θ} is the equilibrium constant at the corresponding temperature, which stands for the dynamic quenching constant (K'_{SV}) in the present paper. The interaction studies were carried out at 298, 304 and 310 K, respectively. The values of K'_{SV}, ΔH^{θ} and ΔS^{θ} were summarized in Table 1. Using the relationship $\Delta G^{\theta} = \Delta H^{\theta} - T\Delta S^{\theta}$, the free energy change (ΔG^{θ}) was estimated as also shown in Table 1. The negative value of ΔG^{θ} revealed that the interaction process was spontaneous. The positive entropy change occurred because the water molecules which were arranged in an orderly fashion around the Au NCs and BSA, acquired the more random configuration as a result of hydrophobic interaction [29]. According to the literature [30], If $\Delta H^{\theta} > 0$, $\Delta S^{\theta} > 0$, the main force is hydrophobic interaction; if $\Delta H^{\theta} < 0$, $\Delta S^{\theta} > 0$, the main force is electrostatic; if $\Delta H^{\theta} < 0$, $\Delta S^{\theta} < 0$, van der Waals and hydrogen bond interactions play major roles in the reaction. In summary, the hydrophobic force contributed the acting between BSA and Au NCs in our study ($\Delta H^{\theta} > 0$, $\Delta S^{\theta} > 0$).

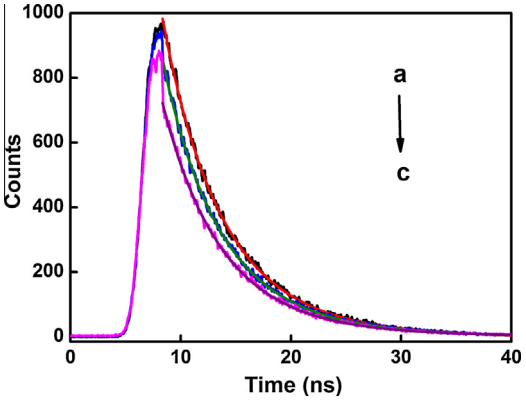

Fig. 6. Fluorescence decay curves showing the decay of (a) 2.00×10^{-5} M BSA, (b) 2.00×10^{-5} M BSA + 1.00×10^{-4} M Au NCs and (c) 2.00×10^{-5} M BSA + 2.00×10^{-4} M Au NCs.

Conformational change of BSA induced by Au NCs

To investigate the possible influence of Au NCs on the secondary structure of BSA, far-UV CD spectra of BSA in the absence and prescence of Au NCs were performed. As show in Fig. 7, the CD spectra of BSA exhibited two negative bands in the UV region at 208 nm and 222 nm. This is a characteristic of an α-helical structure of protein. The peak at 222 nm is contributed by the n–π^* transition of peptide bonds in the α-helix, and the peak at 208 nm is contributed by π–π^* transitions of the peptide bonds on the α-helices [17]. It can be seen that the negative peaks of BSA decreased after addition of Au NCs. Thus, we can deduce that the molecular structure of BSA was changed by Au NCs.

The CD results were expressed in terms of mean residue ellipticity (MRE) in deg cm^2 dmol^{-1} according to the following equation:

$$MRE = \text{Observed CD } (m\,\text{deg})/(C_P n l \times 10) \quad (5)$$

where C_p is the molar concentration of the protein, n is the number of amino acid residues (583 for BSA) and l is the path length (0.1 cm). The α-helical contents of free and reacted BSA were also calculated from MRE values at 208 nm using the following equation:

$$\alpha - \text{helix}(\%) = (-\text{MRE}_{208} - 4000)/(33000 - 4000) \quad (6)$$

as described by Lu et al. [31]. Where MRE_{208} is the observed MRE value at 208 nm, 4000 is the MRE of the β-form and random coil conformation cross at 208 nm and 33,000 is the MRE value of a pure α-helix at 208 nm. From the above equation, the α-helicity in the secondary structure of BSA was determined. The helicity of BSA decreased significantly from 54.3% to 35.2% upon interaction with Au NCs, which suggested a stronger structural change that was related to a low degree of surface coverage.

Furthermore, in order to quantify the different types content of secondary structures, far-UV CD spectra have been analyzed by the algorithm SELCON3. A decreasing tendency of the α-helices content (from 53.8% to 30.4%) and an increasing tendency both of β-strands (from 13.3% to 22.6%) and unordered structure contents (from 22.2% to 36.2%) could be observed. Since the secondary structure contents are closely related to the biological activity of the protein, a decrease in α-helical indicated the loss

Table 1
Quenching constants (K'_{SV}) and thermodynamic parameters for interaction of Au NCs with BSA at 298, 304 and 310 K.

T (K)	K'_{SV} ($\times 10^4$ M^{-1})	R^2	ΔG^{θ} (kJ mol^{-1})	ΔH^{θ} (kJ mol^{-1})	ΔS^{θ} (J mol^{-1} K^{-1})
298	1.31	0.9980	−23.49	35.97	199.53
304	1.53	0.9952	−24.35	35.97	198.42
310	2.32	0.9773	−25.91	35.97	199.61

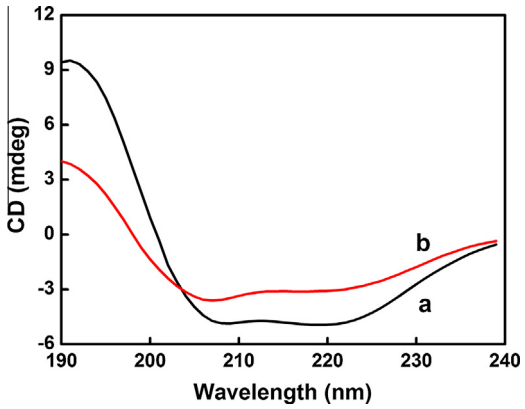

Fig. 7. The far-UV CD spectra of BSA in the absence (a) and presence (b) of Au NCs. The concentrations of BSA and Au NCs were 5.00×10^{-7} M and 1.90×10^{-6} M, respectively.

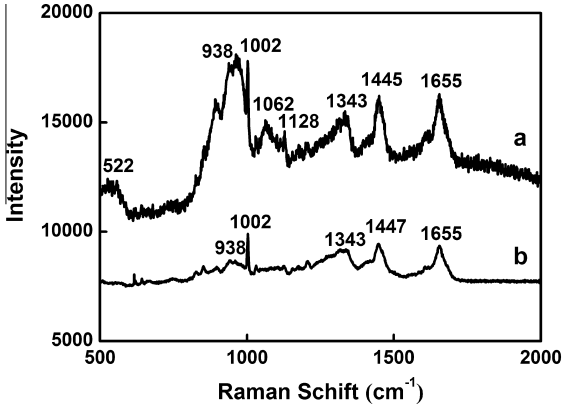

Fig. 8. The Raman spectra of BSA in the absence (a) and presence (b) of Au NCs. The concentrations of BSA and Au NCs were 2.00×10^{-5} M and 2.50×10^{-6} M, respectively.

of the biological activity of BSA upon interaction with Au NCs. The conformation changes here implied that the serum albumin would adopt a more incompact conformation state on the surface of Au NCs and resulted in the exposure of the hydrophobic cavities to the solvent.

Raman spectrum is a good tool to study the interaction of protein and nanoparticles [32]. Fig. 8 depicted the Raman spectra of BSA in the absence (Fig. 8a) and prescence (Fig. 8b) of Au NCs. The 1655 cm^{-1} band mainly resulted from amide I, which is characteristic of high α-helical content in BSA [18]. The intensity decrease at 1655 cm^{-1} indicated that the α-helical content in BSA was reduced after interaction with Au NCs, which is consistent with the CD result. Both the 1002 cm^{-1} band related to the phenylalanine and 1343 cm^{-1} band related to tryptophan or C–H bending were decreased after BSA interaction with Au NCs, showing the exposure of hydrophobic groups of BSA [33]. Thus, the presence of Au NCs could induce structural alterations in the BSA conformation.

Proteins can populate a range of high-energy conformations ranging from local fluctuations to unfolded forms [34]. Many hydrophobic residues play a key role in the native conformation of a protein [35,36]. When histidine-capped Au NCs were added BSA solution under physiological conditions, a hydrophobic force is occurred between BSA and Au NCs. It will lead to disrupt the native conformation of BSA. In addition, the collisions between BSA and Au NCs are the main reason for the quenching of fluorescence of BSA, which also results in the decrease of fluorescence lifetime of BSA.

Conclusions

In this article, we have investigated the interaction between histidine-capped Au NCs and BSA with spectroscopic techniques. It was found that the fluorescence of BSA was quenched by Au NCs at pH 7.4. A dynamic quenching model based on the fluorescence and UV–vis absorption spectra was proved. The thermodynamic parameters, ΔH^{θ}, ΔS^{θ} and ΔG^{θ} were calculated to be 35.97 kJ mol^{-1}, 199.53 J mol^{-1} K^{-1} and −23.49 kJ mol^{-1}, respectively. It was found that hydrophobic force played an important role in the quenching process. Further results from the CD and Raman spectra showed some conformational changes of BSA caused by Au NCs. Such conformational changes could induce toxic effects. Thus, this paper provides new access to explore the potential biology toxicity of Au NCs at the biomolecular level.

Acknowledgments

The authors gratefully acknowledge the support for this research by National Nature Science Foundation of China (20905028), the Fundamental Research Funds for the Central Universities (2011PY009), Natural Science Foundation of Hubei Province Innovation Team (2011CDA115) and Huazhong Agricultural University Scientific & Technological Self-innovation Foundation (2010SC05).

References

[1] J. Zheng, P.R. Nicovich, R.M. Dickson, Annu. Rev. Phys. Chem. 58 (2007) 409–431.
[2] Y.Z. Lu, W. Chen, Chem. Soc. Rev. 41 (2012) 3594–3623.
[3] L.A. Peyser, A.E. Vinson, A.P. Bartko, R.M. Dickson, Science 291 (2001) 103–106.
[4] J.P. Xie, Y.G. Zheng, J.Y. Ying, J. Am. Chem. Soc. 131 (2009) 888–889.
[5] L. Shang, G.U. Nienhaus, Biophys. Rev. 4 (2012) 313–322.
[6] D.H. Tian, Z.S. Qian, Y.S. Xia, C.Q. Zhu, Langmuir 28 (2012) 3945–3951.
[7] K.Y. Pu, Z.T. Luo, K. Li, J.P. Xie, B. Liu, J. Phys. Chem. C 115 (2011) 13069–13075.
[8] Y.L. Wang, Y.Y. Cui, Y.L. Zhao, R. Liu, Z.P. Sun, W. Li, X.Y. Gao, Chem. Commun. 48 (2012) 871–873.
[9] X. Wu, X.X. He, K.M. Wang, C. Xie, B. Zhou, Z.H. Qing, Nanoscale 2 (2010) 2244–2249.
[10] Y. Pan, A. Leifert, D. Ruau, S. Neuss, J. Bornemann, G. Schmid, W. Brandau, U. Simon, W.J. Dechent, Small 5 (2009) 2067–2076.
[11] L. Polavarapu, M. Manna, Q.H. Xu, Nanoscale 3 (2011) 429–434.
[12] L. Shang, N. Azadfar, F. Stockmar, W. Send, V. Trouillet, M. Bruns, D. Gerthsen, G.U. Nienhaus, Small 7 (2011) 2614–2620.
[13] L. Shang, S. Brandholt, F. Stockmar, V. Trouillet, M. Bruns, G.U. Nienhaus, Small 8 (2012) 661–665.
[14] X.Y. Yu, Y. Yang, X. Zou, H.W. Tao, Y.L. Ling, Q. Yao, H. Zhou, P.G. Yi, Spectrochim. Acta A 94 (2012) 23–29.
[15] L. Tang, W.T. Jia, Spectrochim. Acta A 103 (2013) 114–119.
[16] O. Khani, H.R. Rajabi, M.H. Yousefi, A.A. Khosravi, M. Jannesari, M. Shamsipur, Spectrochim. Acta A 79 (2011) 361–369.
[17] L.Z. Zhao, R.T. Liu, X.C. Zhao, B.J. Yang, C.Z. Gao, X.P. Hao, Y.Z. Wu, Sci. Total Environ. 407 (2009) 5019–5023.
[18] Q.Q. Yang, J.G. Liang, H.Y. Han, J. Phys. Chem. B 113 (2009) 10454–10458.
[19] S.H. Lacerda, J.J. Park, C. Meuse, D. Pristinski, M.L. Becker, A. Karim, J.F. Douglas, ACS Nano 4 (2010) 365–379.
[20] X. Yang, M.M. Shi, R.J. Zhou, X.Q. Chen, H.Z. Chen, Nanoscale 3 (2011) 2596–2601.
[21] L. Shang, R.M. Dörlich, V. Trouillet, M. Bruns, G.U. Nienhaus, Nano Res. 5 (2012) 531–542.
[22] B. Hemmateenejad, S. Yousefinejad, J. Mol. Struct. 1037 (2013) 317–322.
[23] J.R. Lakowicz, Principles of Fluorescence Spectroscopy, third ed., Springer, New York, 2006.
[24] L. Shang, Y.Z. Wang, J.G. Jiang, S.J. Dong, Langmuir 23 (2007) 2714–2721.
[25] P.B. Kandagal, J. Seetharamappa, S. Ashoka, S.M. Shaikh, D.H. Manjunatha, Int. J. Biol. Macromol. 39 (2006) 234–239.
[26] Q.S. Wang, X.L. Zhang, X.L. Zhou, T.T. Fang, P.F. Liu, P. Liu, X.M. Min, X. Li, J. Lumin. 132 (2012) 1695–1700.
[27] P. Liu, Q.S. Wang, X. Li, C.C. Zhang, Powder Technol. 193 (2009) 46–49.
[28] R. Mahtab, H.H. Harden, C.J. Murphy, J. Am. Chem. Soc. 122 (2000) 14–17.

[29] A. Sułkowska, M. Maciążek, J. Równicka, B. Bojko, D. Pentak, W.W. Sułkowski, J. Mol. Struct. 834–836 (2007) 162–169.
[30] P.D. Ross, S. Subramanian, Biochemistry 20 (1981) 3096–3102.
[31] Z.X. Lu, T. Cui, Q.L. Shi, Application of Circular Dichroism and Optical Rotatory Dispersion in Molecular Biology, first ed., Science Press, Beijing, 1987.
[32] V.Jr. Tattini, D.F. Parra, B. Polakiewicz, R.N. Pitombo, Int. J. Pharm. 304 (2005) 124–134.
[33] G. Meng, J.C. Chan, D. Rousseau, E.C. Li-Chan, J. Agri. Food. Chem. 53 (2005) 845–852.
[34] D. Wildes, L.M. Anderson, A. Sabogal, S. Marqusee, Protein Sci. 15 (2006) 1769–1779.
[35] I. Lynch, K.A. Dawson, Nanotoday 3 (2008) 40–47.
[36] J.M. Word, S.C. Lovell, T.H. LaBean, H.C. Taylor, M.E. Zalis, B.K. Presley, J.S. Richardson, D.C. Richardson, J. Mol. Biol. 285 (1999) 1711–1733.